AR-009-201

DSTO-TN-0001

Design and Development of a Test Rig for the High Frequency Testing of Rolling Sleeve Airsprings

G. Swanton

DEPARTMENT OF DEFENCE
DEFENCE SCIENCE AND TECHNOLOGY ORGANISATION

Design and Development of a Test Rig for the High Frequency Testing of Rolling Sleeve Airsprings

G. Swanton

Airframes and Engines Division
Aeronautical and Maritime Research Laboratory

DSTO-TN-0001

ABSTRACT

AMRL's F/A-18 IFOSTP fatigue test has introduced several new concepts in the field of aircraft structural testing. One of the innovations has been the development of the pneumatic actuator or "rolling sleeve" airspring for the application of aircraft manoeuvre loads. These airsprings have been subjected to several preliminary acceptance test phases, one of which simulated the effects of high frequency buffet loads. This report details the design and implementation of the test rig developed to conduct this type of testing.

Approved for public release

DEPARTMENT OF DEFENCE

DEFENCE SCIENCE AND TECHNOLOGY ORGANISATION

Published by

DSTO Aeronautical and Maritime Research Laboratory
PO Box 4331
Melbourne Victoria 3001 Australia

Telephone: (03) 626 7000
Fax: (03) 626 7999

AR No. 009-201
February 1995

APPROVED FOR PUBLIC RELEASE

Design and Development of a Test Rig for the High Frequency Testing of Rolling Sleeve Airsprings

EXECUTIVE SUMMARY

The RAAF and Canadian Forces (CF) have embarked on a collaborative full-scale F/A-18 fatigue test known as the International Follow-On Structural Test Program (IFOSTP), with AMRL performing the testing of the aft fuselage and empennage, and the Canadians testing the central fuselage and wings.

The IFOSTP project does not use the conventional "whiffle-tree" method of loading aircraft during full-scale structural testing. Instead, AMRL has designed and developed another means of applying aircraft manoeuvre loads:- the "rolling sleeve" airspring. These airsprings have a relatively low stiffness and mass compared to a whiffle-tree system and hence contribute less to these characteristics of the test article. The differential pressure in a pair of rolling sleeve airsprings distributed over the structure imparts the desired load distribution into the structure. The pressurisation causes these inflatable fabric cylinders to move up and down with a rolling action along their support stands.

Three different phases of airspring testing have been devised: 1) static strength testing, 2) durability testing under manoeuvre loading and 3) durability testing under dynamic buffet loading. This report describes the development of a test rig for the phase 3 testing. The test rig was designed using a finite element computer package as well as an analytical solution to confirm the results. The working of the analytical approach to this particular application is one not widely presented in texts and so has been described in this report.

Contents

1. Introduction

The DSTO Aeronautical & Maritime Research Laboratory (AMRL) has developed a unique system for the application of manoeuvre loads to aircraft test articles. As a replacement for the more conventional hydraulic jacks used in previous structural tests, low stiffness pneumatic actuators, known as "rolling sleeve" airsprings (or airbags) have been designed and developed to apply aircraft manoeuvre loads. Although manufacturing techniques and selection of suitable materials is an ongoing evolutionary process, specific airspring units once made, must satisfy test requirements to verify their suitability for use in terms of strength, durability and dynamic operating characteristics. This airspring loading system will be first trialed on the empennage structure of the IFOSTP full scale F/A-18 fatigue test article. (Reference 1).

Fatigue testing of the AMRL F/A-18 test article will not only simulate manoeuvre loading, but also the high frequency dynamic loading (or "buffet") that the aircraft experiences under certain flight conditions. In order to gauge how the airsprings will react to the differing load cases, independent tests have been established to test different airspring designs. Three tests have been devised; a static strength test, a manoeuvre load simulation test, and a buffet simulation test which subjects the airsprings to high frequency and small displacements. This report addresses the latter requirement.

Although AMRL had available a customised horizontal stabilator rig that was initially used for developing the airspring loading system, for reasons of time, cost and ease of manufacture, a simple cantilevered beam structure was chosen for the continuation of this task, to be vibrated in its fundamental bending mode by an electromagnetic shaker. It should be noted that the main aim in sizing the rig was to achieve a certain prescribed tip deflection at the end of the beam at a prescribed frequency. Another testing requirement of this phase of test was to determine the damping characteristics of different kinds of airbags, which meant that the rig also had to cater for "free vibration" damping tests.

This report gives a brief background outlining the testing methodology developed for AMRL's F/A-18 IFOSTP and the need to test the airbag system. It then focuses on the design of the high frequency, low displacement test rig, presenting the classical approach for the derivation of the equations of motion of a cantilever beam undergoing periodic motion.

2. IFOSTP Testing Methodology

During F/A-18 flight, there are many instances when significant empennage manoeuvre loads occur simultaneously with high buffet activity, causing structural damage to the aircraft's aft region - see Reference 2. In order to accurately simulate this environment on a test article, a unique test system has been developed. The testing at AMRL will simulate the aircraft manoeuvre loads (distributed aerodynamic loads & inertia loads) by using a new airbag (or airspring) loading arrangement

instead of the more conventional hydraulic loading and contour board/pad system (collectively known as a "whiffle-tree" arrangement). Because the airsprings have a relatively low spring stiffness and mass compared to the whiffle tree, much less stiffness and mass will be added to the structure, minimising the effect on the dynamic characteristics of the structure, thus allowing the structure to be excited near its natural resonant frequencies.

These airsprings consist of an opposing pair - one on either side of the structure, the loading of the airspring pair being determined by the differential pressure between the airbags. Air reservoirs of sufficient volume are used in conjunction with the airsprings to provide structural support and to minimise the effective spring stiffness of the system (stiffness of an airspring is inversely proportional to its volume). The dynamic buffet conditions are reproduced using high powered, high displacement electromagnetic shakers.

There are several types of airsprings that will be used for the application of manoeuvre loads. One of these types of actuators is the convoluted or "bellows" type commercial airspring (see Figure 1 overleaf) - these are used in the pneumatic suspension systems of trucks and for isolating machinery and equipment from other structures in a vibrational environment. They are manufactured by Firestone and come in various diameters.

Development testing using these commercial actuators found them inadequate for the outer tip areas of the fins and stabilators as they added too much stiffness, causing an unacceptable increase in modal frequencies. The commercial airsprings also had trouble meeting the large tip deflections experienced during loading. This necessitated the development of the "rolling sleeve" airspring/actuator. The development of the rolling sleeve airbag is detailed in Reference 3. These low stiffness airsprings (approx. 1/3 stiffness of the commercial type) were originally manufactured from a Kevlar/MYLAR sail cloth material and were fitted to large volume reservoirs. These had very low durability due to the MYLAR cracking and then abrading the Kevlar.

Further development work led to the trial of different airbag materials in a bid for improved characteristics such as durability, flexibility, strength and air-tightness. The next prototype consisted of a cylinder of latex coated kevlar which was stitched and sealed. These were followed by neoprene coated kevlar that was stitched then cured in an autoclave. Current airbags consist of a PVC coated polyester weave and have a welded seam (high frequency heat bonding process that fuses the airbag coating together). All bags are capped at one end. Tucks are made around the open end to achieve a reduction in diameter to suit the connection to the reservoir upstand support. The usual upstand support for the airsprings is a length of 10.79 inch[1] (274 mm) outer diameter steel tubing (but can vary depending on airbag diameter).

Early experience from tests conducted at AMRL showed that failure of the airbags tended to occur at creases in the fabric caused by the seam or tucks during the rolling action. Subsequently, a corrugated plastic sleeve was introduced to reduce the creasing at the roll by increasing the perimeter of the reservoir upstand so that it is closer to that of the airbag. A rolling sleeve airspring is shown in Figure 2.

[1] IFOSTP convention is to use imperial units.

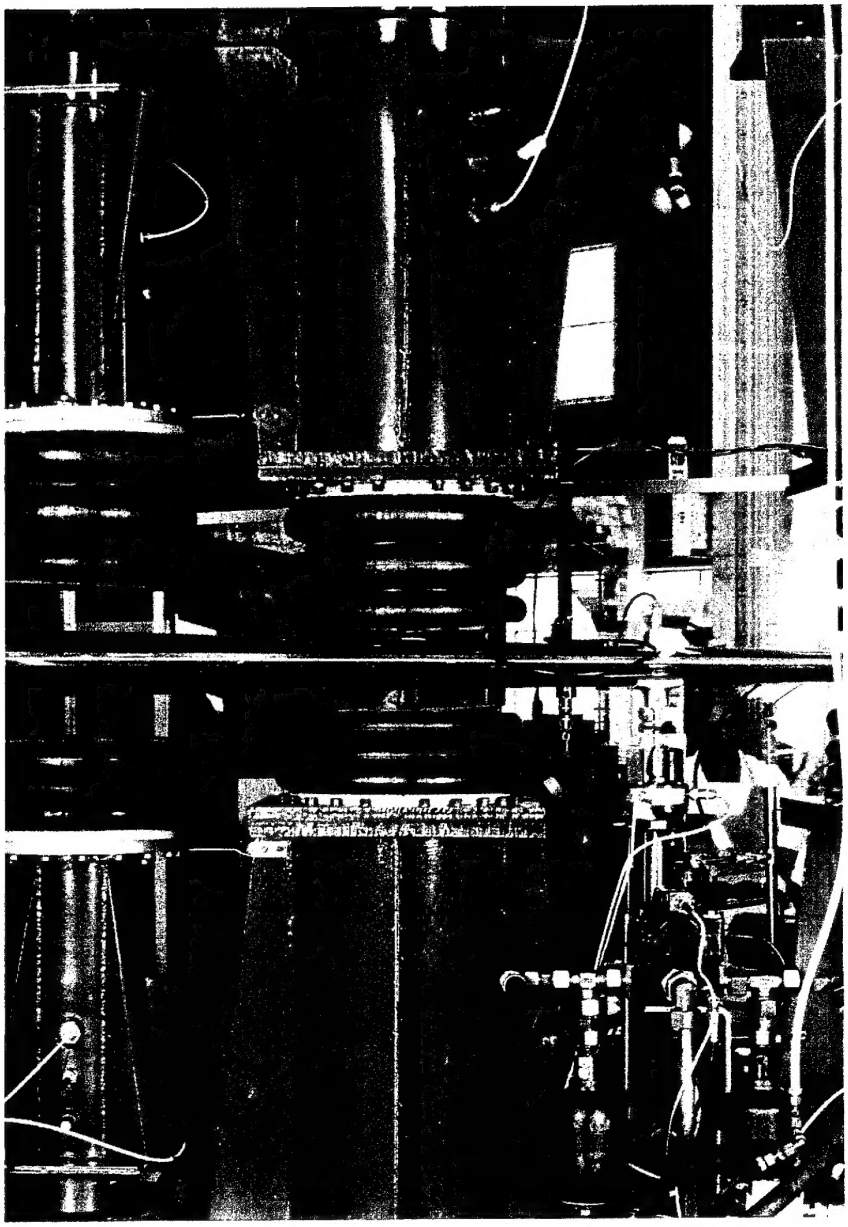

Figure 1: Commercial type of airspring applied to horizontal stabilator.

The design requirements for the airsprings to meet the IFOSTP specifications are:

Maximum working pressure:	40 psi (275 kPa)
Peak System Pressure	50 psi (345 kPa)
Design maximum load:	4635 lbf (20.6 kN)
Airspring outer diameter:	13.5 inches (343 mm)
Durability:	120,000 cycles from 350 lbf to 1740 lbf (1.5 kN to 7.75 kN)
	2,000,000 cycles of 1 inch (25 mm) stroke at 1740 lbf (7.75 kN)
Stroke:	16 inches (406 mm)
Media:	Compressed air and oil mist.

This page intentionally left blank

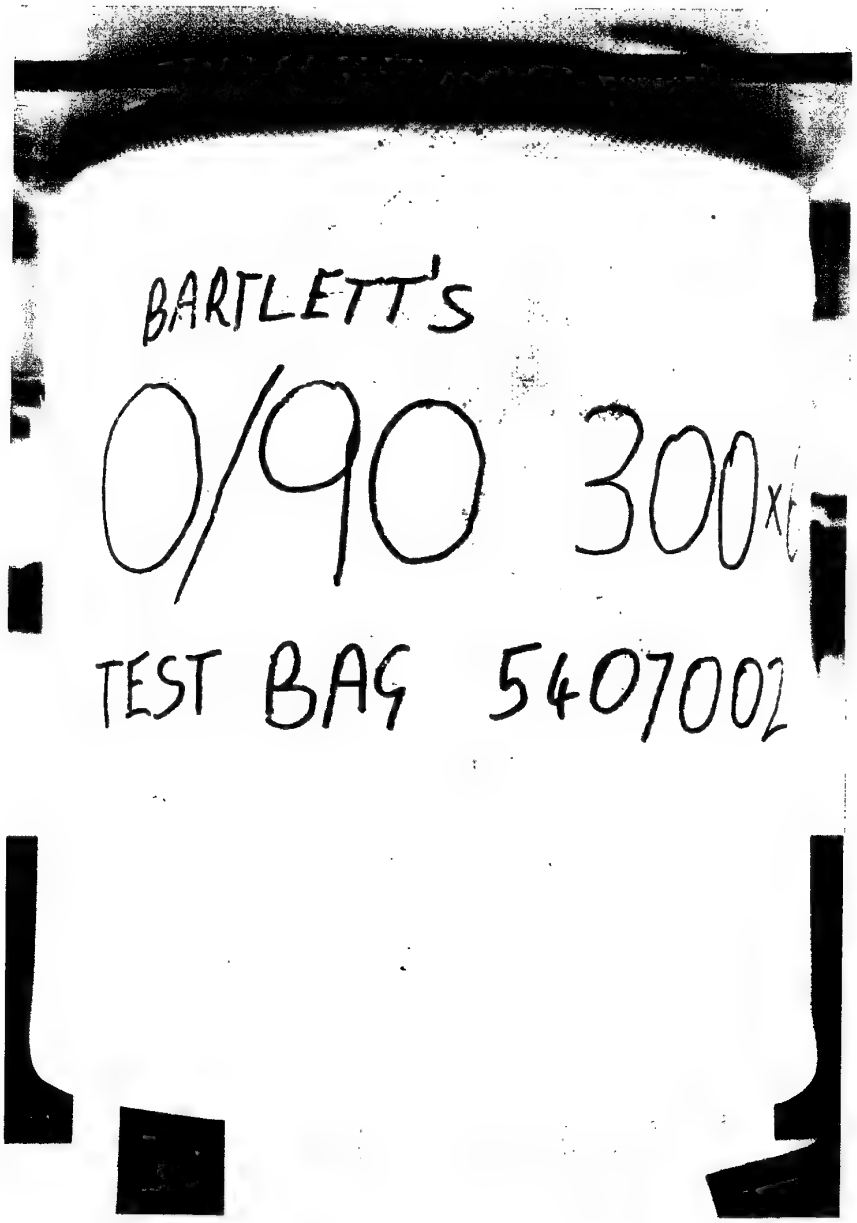

Figure 2: An example of a current rolling sleeve airspring.

3. Test Requirements

The airsprings, when in use during the IFOSTP testing, will be controlled via a control law which pressurises the "loading" airspring while the opposing airspring is to be kept at a nominal 3 psi pressure. During manoeuvre loading, the deflection of the flight surfaces will be in the direction of loading, subjecting the airsprings to a combination of pressurisation stressing and the wearing effects of the rolling action. At certain intervals, while under constant load, the structure, and hence airsprings, will be subjected to the high frequency buffet simulation. In these instances, "wear" of the airsprings will be due to the displacement caused by the rolling action only, and not due to major cyclic pressure changes on the body of the airspring.

Buffet Loads: Having withstood phase 1 and phase 2 airspring development testing, the airsprings are then subjected to the high frequency, small displacement, constant amplitude test. Test requirements are for airsprings to be inflated to apply a 1740 lbf static load with endcap displacement of ±1 inch for 2,000,000 cycles[2].

To realise these requirements, the working section of the test rig was designed to have a natural frequency of approximately 15 Hz so as to coincide with the 15 Hz primary bending mode of the F/A-18 vertical tail - this meant that minimal force input would be needed to drive the rig at (or near) resonance. The endcap displacement of ± 1 inch was thought to be sufficient to observe the effects of deflection on the rest of the airbag. The loading system used to achieve this was an electromagnetic shaker with a 1000 lbf capability.

Damping: Another test requirement was to measure the damping effects of different airsprings to test their suitability for use on the IFOSTP rig. A comparative test was devised whereby the working section of the test rig would be made to vibrate naturally with and without various airspring pairs attached - the method of determining the damping is described in section 6.2.

An airspring passing the above criteria[3] should be able to withstand at least one test block of loading on the IFOSTP rig.

---

[2] The 2,000,000 cycles of phase 3 testing was derived by determining from F/A-18 operational data (SPEC6G), the total time spent when the angle of attack (AOA) > 28° and dynamic pressure (Q) > 75 psf, and choosing rolling sleeve airspring location 47 (stbd) or 57 (port) on the vertical tails as having the severest average displacement environment resulting primarily from mode 1 response to buffet.

The total time spent within this AOA-Q region was 2828 seconds per flight block. Since the average mode 1 frequency expected for the fatigue test is 17 Hz, and the number of blocks for two aircraft lifetimes is 40, the total number of mode 1 cycles = 1,923,108. This was rounded upwards to give 2,000,000 cycles. From the Canadian Aerospace Engineering Test Establishment (AETE) PD88/12 flight response measurements, the average mode 1 response at McAIR measurand locations KS16/KT16 (vertical tail, rear tip, port & stbd respectively) for the above AOA-Q region was determined as 23.76 g rms, and the corresponding response for KS01/KT01 (vertical tail, forward tip, port & stbd respectively) was 13.70 g rms. Knowing the position of the airspring relative to these transducer locations, the average mode 1 response at the airspring was determined to be approximately 19 g rms. Assuming this response to be a very narrow band centred at 17 Hz, the expected peak displacement would be ± 0.91 inches. Hence an endcap displacement of ± 1.0 inch was chosen for this test.

[3] The airbags had to survive at least one full block of loading (≅ 300 hrs), but preferably much longer.

Besides meeting the above criteria, it should be noted that the construction, operation, performance and versatility of the test rig were also major points for consideration. Low cost of new materials, availability of in-house equipment and ease of manufacture were the driving factors behind the construction of the rig. An operating system that required minimal human assistance was implemented to allow for extended usage for operator free running periods such as overnight running. The test rig itself had to perform predictably as well - therefore it needed a solid foundation and a working section that was not prone to erratic behaviour or failure.

4. High Frequency Test Rig Design

A cantilever beam was chosen as the design best suited to fulfil the test requirements. However, as only the fundamental bending mode (in the vertical direction) was being investigated in the actual test, it was important that the beam be stable against torsional and sideways modes which might occur at frequencies close to the vertical mode (~ 15 Hz). Therefore, a rectangular tube section was used as its characteristics best suited these requirements. A simple uniform cantilever beam (no tip masses), utilising a particular beam section that was readily available, was chosen for the initial design stages of the rig, and its details are shown in Figure 3. The beam length of 70 inches is purely arbitrary.

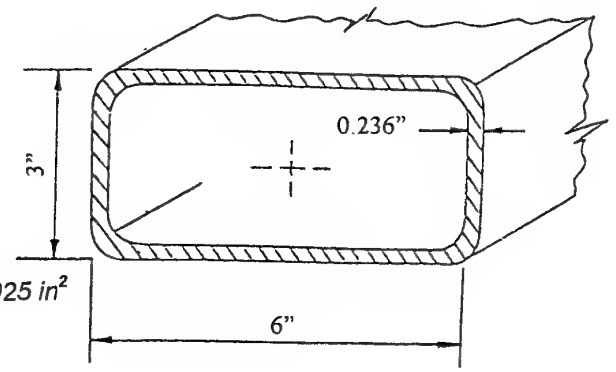

MATERIAL: mild steel
CROSS SECTIONAL AREA, A = 4.025 in^2
LENGTH = 70 in
E = 29 x 10^6 psi
ρ = 0.283 lb/in^3
I = 6.057 in^4
g = 386 in/s^2

Figure 3 : Beam characteristics used for initial stages of design work.

Design of the airspring test rig was performed using two techniques. One method utilised the dynamics capability of the PAFEC finite element model (FEM) package and the other method utilised an analytical solution approach. In order to optimise the dimensions of the rig (to obtain the prescribed displacements and check stresses), sizing of the cantilever was performed using the FEM, as it provided a quick and straightforward means of experimenting with such parameters as beam geometries, material properties and force inputs.

However, in the initial stages of design work, an analytical solution for finding the displacements of beams undergoing forced harmonic motion was also utilised, so that some confidence could be gained from the results given by the FEM. The next two sections present details on both of the methods used to design the rig. A comparison of the results from the two techniques using the beam described above is presented in section 4.3.

4.1 PAFEC FEM Approach

The PAFEC suite of software was used to solve for the beam displacements and natural frequencies. The input file for the FEM solution for an initial example test run is shown in Appendix 1.

The geometry of the cantilever beam was defined along with the type of element chosen to represent the structure in the "NODES" and "ELEMENTS" modules respectively. In this case simple beam elements totalling a length of 70 inches were used. It should be noted that the lengths and number of these beam elements is variable. If a different beam section is required, the dimensions of the beam elements can be modified in the "BEAMS" module to represent different beam geometries. The material properties of mild steel were specified in the "MATERIAL" section. In the remaining modules, the direction of displacement was restricted to the vertical only, with the built-in end of the cantilever being restrained in every direction. Also the value and location of the applied force, the amount of critical damping and output information was specified for various runs.

Because the time to run a complete analysis on the job was short (in the order of a few minutes), many changes were made to one parameter at a time, checking the resulting displacements, frequencies and stresses.

For this example, the force input (ie: position of electromagnetic shaker) was set at 36 inches from the built-in end, corresponding to Node #10 in the FE model. The displacement output files shown in Appendix 2 are for applied forces of 600 lbf and 1000 lbf.

4.2 Analytical Approach

This section presents the analytical formulation for the vertical displacements of a cantilever beam undergoing forced vertical vibration, excited by a concentrated load acting in the vertical direction at an arbitrary point within the beam span. The reference axes and configuration are shown in Figure 4.

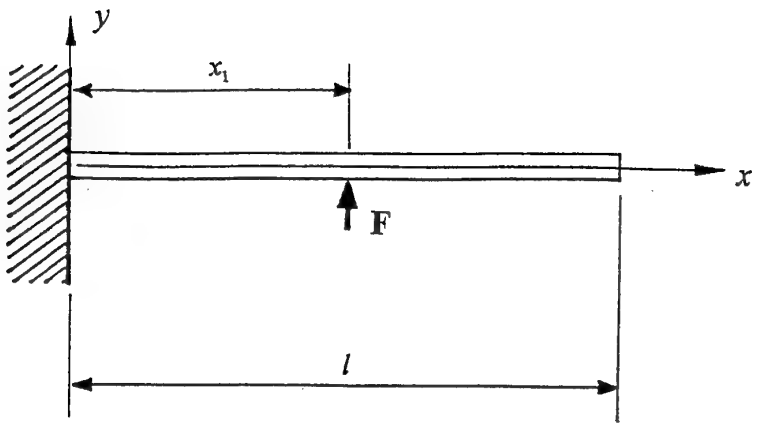

Figure 4: Axis system and notation.

The formulation of the problem is presented below:

The differential equation (DE) for the flexural vibration of a beam has the following form (from Reference 4) and is valid for 0 < x < l:

$$-\frac{\partial^2}{\partial x^2}\left[EI(x)\frac{\partial^2 y(x,t)}{\partial x^2}\right]+f(x,t)=m(x)\frac{\partial^2 y(x,t)}{\partial t^2} \qquad (1)$$

with $f(x,t)$ being the force per unit length. The solution to the DE in terms of displacement, y, as a function of distance along the beam (x) and time (t), is assumed to be of the following form:

$$y(x,t)=Y(x)\cdot F(t) \qquad (2)$$

where $Y(x)$ represents the mode shape of the beam and depends on the spatial variable x alone, and where $F(t)$ is the generalised coordinate indicating the amplitude of motion the beam executes with time and depends on t alone.

Then for the case when $f(x,t)=0$ we have:

$$-\frac{EI}{m}\frac{Y''''}{Y}=\frac{\ddot{F}}{F}=-\omega^2 \qquad (3)$$

where m is the mass of the system and ω is the frequency of $F(t)$, assuming that $F(t)$ is sinusoidal. Thus, the eigenvalue problem, associated with a beam in bending vibration is of the form of the following differential equation:

$$\frac{d^2}{dx^2}\left[EI(x)\frac{d^2 y(x,t)}{dx^2}\right]=\omega^2 m(x)Y(x) \qquad (4)$$

$EI(x)$ is referred to as the flexural rigidity and $m(x)$ the mass per unit length at any point x along the beam. In the case of a uniform beam, EI and m are constant, and equation (4) reduces to:

$$\frac{d^4Y(x)}{dx^4} - k^4Y(x) = 0 \tag{5}$$

where the term k is defined by:

$$k^4 = \frac{\omega^2}{a^2} \tag{6}$$

and the constant a is defined as:

$$a = \sqrt{\frac{EI}{m}} \tag{7}$$

The general expression for a normal function can be written as (from Reference 5):

$$\begin{aligned} Y_i(x) &= C_1(\cos k_i x + \cosh k_i x) + C_2(\cos k_i x - \cosh k_i x) \\ &+ C_3(\sin k_i x + \sinh k_i x) + C_4(\sin k_i x - \sinh k_i x) \end{aligned} \tag{8}$$

where C_1, C_2, C_3 and C_4 are constants of integration. Hence the derivatives of $Y_i(x)$ can be determined and these are presented in Appendix 3. The boundary conditions are:

$$\begin{aligned} (Y)_{x=0} &= 0 \\ (Y')_{x=0} &= 0 \\ (Y'')_{x=l} &= 0 \\ (Y''')_{x=l} &= 0 \end{aligned} \tag{9}$$

Using the expressions for normal functions from Appendix 3 (derived from eqn. (8)) and properties of hyperbolic functions given in Appendix 4, the following frequency equation can be obtained from (8):

$$\cos kl \cosh kl = -1 \tag{10}$$

The first six roots of equation (10) are as follows:

$$\begin{aligned} k_1 l &= 1.875 \\ k_2 l &= 4.694 \\ k_3 l &= 7.855 \\ k_4 l &= 10.996 \\ k_5 l &= 14.137 \\ k_6 l &= 17.279 \end{aligned} \tag{11}$$

(NOTE: Should the roots for higher modes be required, they may be approximated by the following formula from the curve derived from equation (10) as shown in Appendix 5):

$$k_i l \approx \frac{2i-1}{2}\pi \tag{12}$$

Applying the boundary conditions of (9), the equation for the cantilever (8) becomes:

$$Y_i(x) = B_i\left[(\cos k_i x - \cosh k_i x) + \alpha_i(\sin k_i x - \sinh k_i x)\right] \tag{13}$$

where:

$$\alpha_i = -\frac{\cos k_i l + \cosh k_i l}{\sin k_i l + \sinh k_i l} \tag{14}$$

and constants B_i are selected to satisfy the conditions of normalisation:

$$\int_0^l Y_i^2(x)dx = 1 \tag{15}$$

ie:
$$B_i = \frac{1}{\sqrt{\int_0^l\left[(\cos k_i x - \cosh k_i x) + \alpha_i(\sin k_i x - \sinh k_i x)\right]^2 dx}} \tag{16}$$

It is possible to obtain the expression for the response $y(x,t)$ caused by the concentrated force $P_1(t)$, in the form (See Reference 5):

$$y(x,t) = \sum_{i=1}^{\infty} \frac{Y_i Y_{i1}}{\omega_i}\int_0^t \frac{P_1(t')}{m}\sin\omega_i(t-t')dt' \tag{17}$$

where ω_i is the i^{th} natural frequency, and Y_{i1} is Y_i evaluated at the location of P_1. Assuming that the vibrations are produced by a harmonic force $P_1(t) = P\sin\Omega t$, where Ω is the driving frequency, then:

$$\begin{aligned} y(x,t) &= \frac{P}{m}\sum_{i=1}^{\infty}\frac{B_i^2}{\omega_i^2}\left[(\cos k_i x - \cosh k_i x) + \alpha_i(\sin k_i x - \sinh k_i x)\right] \\ &\quad \times\left[(\cos k_i x_1 - \cosh k_i x_1) + \alpha_i(\sin k_i x_1 - \sinh k_i x_1)\right]\int_0^t \sin\Omega t' \sin\omega_i(t-t')dt' \\ &= \frac{P}{m}\sum_{i=1}^{\infty}\frac{B_i^2}{\omega_i^2}\left[(\cos k_i x - \cosh k_i x) + \alpha_i(\sin k_i x - \sinh k_i x)\right] \\ &\quad \times\left[(\cos k_i x_1 - \cosh k_i x_1) + \alpha_i(\sin k_i x_1 - \sinh k_i x_1)\right]\left(\sin\Omega t - \frac{\Omega}{\omega_i}\sin\omega_i t\right)\beta_i \end{aligned} \tag{18}$$

where the magnification factor β_i is given by:

$$\beta_i = \frac{1}{1-\Omega^2/\omega_i^2} \tag{19}$$

The first part of equation (18) represents steady-state forced vibrations of the beam, whereas the second part consists of transient free vibrations. For this particular application, only the steady-state response will be of practical importance.

Alternatively, using $ma^2 = EI$, where a was defined in (7), and the natural frequency being given by equation (6), then:

$$\omega_i = k_i^2 a = (k_i l)^2 \sqrt{\frac{EI}{ml^4}} \tag{20}$$

and the response may then also be expressed thus:

$$y(x,t) = \frac{P}{EI} \sum_{i=1}^{\infty} \frac{B_i^2 l^4}{(k_i l)^4} \left[(\cos k_i x - \cosh k_i x) + \alpha_i (\sin k_i x - \sinh k_i x) \right] \times \left[(\cos k_i x_1 - \cosh k_i x_1) + \alpha_i (\sin k_i x_1 - \sinh k_i x_1) \right] \left(\sin \Omega t - \frac{\Omega}{\omega_i} \sin \omega_i t \right) \beta_i \tag{21}$$

So, with B_i, α_i and k_i being the only quantities to calculate separately (the rest being specific inputs), the displacement y at position x and time t can now be determined. A tabulated form for the solution of equation (21) is set out in Appendix 6.

In order to calculate the displacements of the system, the natural frequencies also had to be determined. Using a variation of equation (20) above, the results are listed in Column 8 on the table in Appendix 6. The mass per unit length m has been substituted for $\rho A/g$ and the final result is multiplied by $1/2\pi$ to give units in hertz. The equation for the first mode is shown below:

$$\omega_1 = \frac{3.52}{l^2} \sqrt{\frac{EIg}{\rho A}} \cdot \frac{1}{2\pi} \quad \text{(Hz)} \tag{22}$$

It should be noted that the results from the analytical solution derived above do not account for damping (note that the natural frequency of the system is independent of damping) - therefore, to keep things consistent, the FEM file (Appendix 1) also had zero damping. The results for two force inputs were tested - 600 lbf and 1000 lbf.

4.3 Results

A comparison of tip deflections for two different applied loads (600 lbf and 1000 lbf) at several forcing frequencies is presented in Table 1. The first entry in each cell is from the FE solution and has been taken directly from the highlighted sections of Appendix 2. The second entry (in parenthesis) is from the analytical solution of equation (21) and has been calculated as per the example in Appendix 6.

Table 1: Comparison of displacements (in inches) from the FE and analytical solutions.

	Ω = 3 Hz	Ω = 10 Hz	Ω = 15 Hz	Ω = 23 Hz	Ω = 27 Hz	Ω = 30 Hz	Ω = 35 Hz
P = 600 lbf	0.1299 (0.1299)	0.1473 (0.1482)	0.1800 (0.1834)	0.3797 (0.4171)	1.299 (2.2141)	1.270 (-0.8532)	0.2735 (-0.2404)
P = 1000 lbf	0.2165 (0.2165)	0.2455 (0.2470)	0.3000 (0.3056)	0.6329 (0.6951)	2.165 (3.6899)	2.117 (-1.4219)	0.4559 (-0.4006)

One can see that the comparison appears favourable, especially with values extracted at frequencies distant from resonance. For example, with a shaker force of 1000 lbf and a driving frequency of 10 Hz, the FE solution gives a tip displacement (at node #19 - see schematic in Appendix 1) of 0.2455 inches while the analytical method gives 0.2470 inches. Also, some of the analytical results are negative - however, it is the magnitude which is of interest.

Another point to note is that the analytical calculation (eqn. (22)) produced a fundamental natural frequency of 27.86 Hz while the FEM solution calculated this quantity as 28.51 Hz. The FEM result of the natural frequency calculation is displayed in the PAFEC frequencies and displacements output file - however this output file is very large and has been edited to only show the displacements as presented in Appendix 2. The biggest differences between the two methods occurs near resonance - however, regardless of which method is used, the largest displacements are found to occur at this point (resonance). Some possibilities that may contribute to the discrepancies (ie: differences in natural frequency) are:

- differences due to rounding errors,
- the accuracy of the FEM solution is affected directly by the complexity ofthe model. Errors are introduced depending on the level of model refinement, as well as the choice of other output-analysis modules.

With both sets of data showing general agreement for the simplified test case, this indicated that the FEM results could be used with confidence to proceed with a more detailed rig design.

5. Test Rig Configuration

The "final" version of the cantilever was chosen to have a natural frequency of around 15 Hz - to coincide with the 15 Hz primary bending mode excitation of the F/A-18 vertical tail. The provision for a surface on which to react the airspring pair was needed, so it was decided to make this surface from half inch steel plate and attach it to the free end of the cantilever. The dimensions of this plate were fixed - it had a certain thickness and it had to be big enough to support the endcaps of the airsprings. Consequently, this was a fixed parameter in the FEM (the plate was still modelled as a beam element but with sectional properties representative of the plate). Then the beam length was altered until the target natural frequency of 15 Hz was achieved. The same beam section as described in the example case was used as it provided good

results and was readily obtainable. The position of the electromagnetic shaker (ie: force input) was also varied to find an optimum location giving the required tip deflections. This resulted in an overall cantilever length of 84 inches - a 70 inch beam with a 14 inch plate at the end. The shaker position was at 36 inches from the built-in end.

When constructing the rig, the following method of fixation to simulate a cantilevered structure was used: A 2 ton concrete block (48 inches long, 30 inches wide and 36 inches high) was chosen as a base on which to attach the beam for several reasons - it provided a solid and compact foundation, as well as being a suitable height that required little modification to accommodate the shaker. On top of the concrete block was bolted a one and one quarter (1.25) inch thick steel plate. As a result, when it came to ordering the beam from the supplier, an extra 48 inches was added to the length of the beam, giving an overall length of 118 inches. This extra 48 inch section was attached along the whole length of the upper surface of the steel plate. Pieces of angle-section were then welded either side of the beam and onto the steel plate. The concrete block was also anchored to the floor using heavy channel-sections to prevent motion induced during dynamic loading.

The steel "pad" at the free end of the beam was actually 20 inches in length - a 6 inch cutout at the end of the beam was made so that the pad could be slotted in and welded into place, hence leaving a 14 inch overhang.

A small bracket was also welded to the underside of the beam between the built-in end and shaker. This served as the point from which the beam could be "jacked" down and released for the free vibration damping tests. Refer to Figure 5.

Although not part of the rig design, a support frame to house the airbag reservoirs, mounts, gauges and tubing was also constructed at the free end of the beam.

5.1 Test Rig Equipment & Instrumentation

The initial test rig set-up and associated control devices consisted of the following items:

TEST RIG COMPONENTS

* mild steel box-beam section (6 x 3 x .236 in, 118 inches long),
* steel plate ("end pad") - for airsprings to support against (20 x 14 x 0.5 in.),
* 2 ton concrete block - as an attachment point for cantilever,
* steel base plate - beam attachment surface on top of concrete block (48 x 30 x 1.25 in.),
* upright support stands - for airspring and reservoir installation,
* 1 pair of rolling sleeve airsprings and associated air reservoirs & fixtures,
* pressure transducers and gauges - to regulate and monitor pressure in airsprings,
* hand operated hydraulic jack and Canberra bomb release - to draw beam downwards and release it for free vibration damping tests.

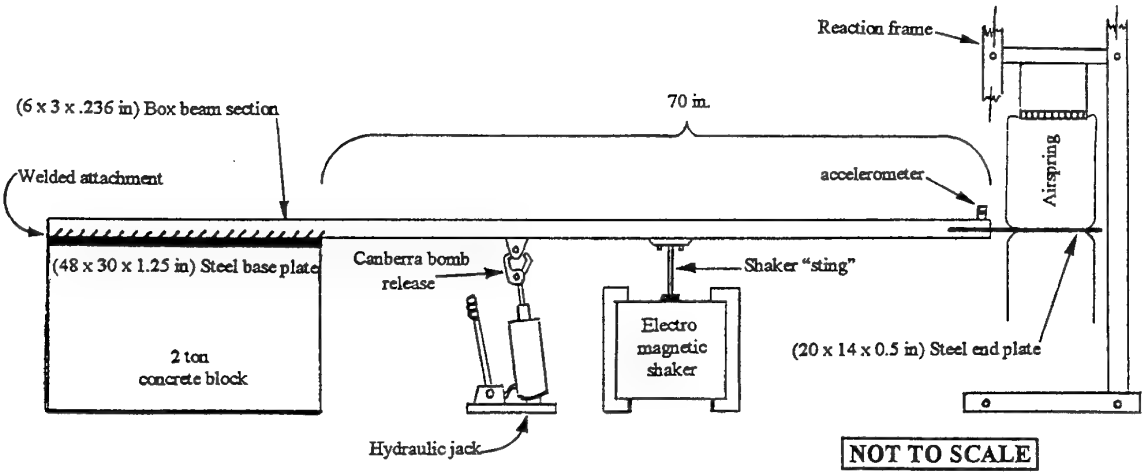

Figure 5: Schematic of original test rig set-up.

LOADING SYSTEM & CONTROLLER

* **OZY-DYN** signal generator - sets the driving frequency & displacement input signal,
* **LING** 1000 lbf electromagnetic shaker & amplifier - the amplifier magnifies the low power input from the signal generator to an operational level for the shaker.

INSTRUMENTATION

* Kistler accelerometer - to measure tip acceleration with respect to time,
* Nicolet cathode ray oscilloscope (CRO) - to capture accelerometer trace,
* Wavetek signal filter - used to filter out higher frequency modes in damping test,
* displacement recorder/plotter - provides a visual indication that specified amplitude is being maintained,
* digital counter - to determine completion of 2 million cycles.

6. Testing Procedure

6.1 Durability Testing

The pair of rolling sleeve airsprings under test were attached as shown in the above figure and pressurised to 5 psi before exciting the beam. For the high frequency testing, the shaker "sting" (the shaft transmitting the force output), was attached to the underside of the beam. The LING amplifier was then powered up which in turn started the electromagnetic shaker. Using a frequency set control on the signal generator (which provided the inputs for the amplifier), the shaker was then set to vibrate the beam near resonance (~ 15 Hz). An accelerometer positioned at the end of the beam (just in front of the upper airspring) was used in a feedback loop to prevent drifting of the set frequency. Another control on the signal generator was used to

achieve the desired displacements. Once the test was running, this arrangement allowed for unmanned operation, although periodic inspections were conducted to ensure the equipment was operating normally. The rig showed no signs of instability.

The testing spectra consisted of cycling the airsprings, with static tests and load versus pressure tests being performed at various intervals until the 2 million cycles were achieved.

6.2 Damping Testing

When the rig was used for the damping tests, the shaker sting was disconnected and the hand operated hydraulic jack (with Canberra bomb release attached to end) was then linked up to a connecting pin on the underside of the beam. The jack was then used to draw the beam downwards 1 inch before setting off the bomb release, causing free vibration of the beam. The displacement trace was captured on the CRO, using the same accelerometer as mentioned before. Measurements were taken of the trace to determine damping and frequency. Damping was determined by using the displacement amplitude ratios and chart shown in Figures 6 and 7, and as described in Reference 6. (For example, if $x_3 / x_0 = 0.7$, then read off the n=3 curve to obtain 0.019 or 1.9% damping).

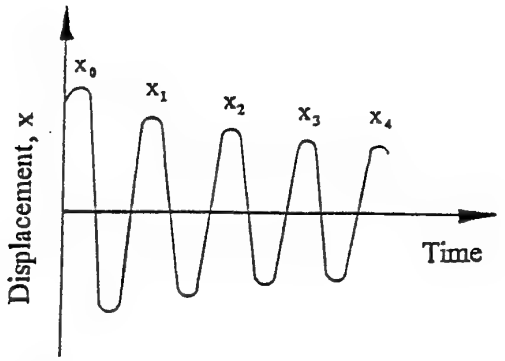

Figure 6: CRO displacement trace.

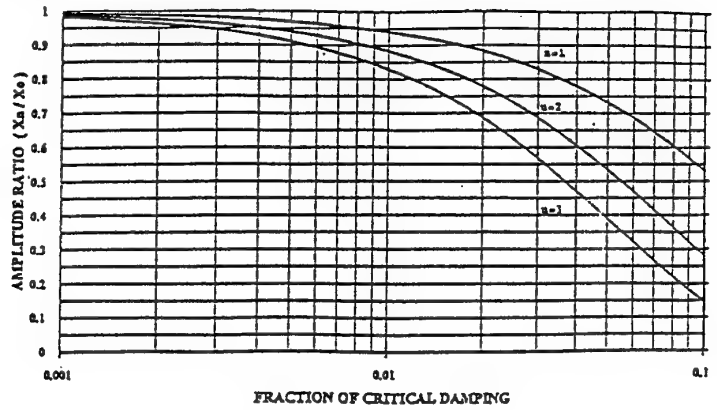

Figure 7: Amplitude ratio vs. Fraction of critical damping.

The natural frequency of the system was calculated by measuring the duration of one cycle (in seconds) from the CRO display, then taking its inverse. (For example, when the beam was vibrated without any airbags attached, there was a time interval of 0.075 seconds between x_1 and x_2 - this gave a natural frequency of 1/0.075 = 13.33 Hz.).

7. High Frequency Test Results

The first pair of airsprings to successfully complete the 2 million cycles were constructed from a vinyl coated polyester fabric (weave direction 90/0) manufactured by Polymar (type number 8556). However, these particular airsprings had not been subjected to phase 2 testing (they were subjected to phase 1 testing, as are all specimens). They were then statically tested again to 40 psi and showed no signs of degradation[4]. The values of damping ranged from 1.8% of critical at 5 psi to 2% of critical at 15 psi.

The next set of airsprings tested were made from the same material but were of a heavier gauge (type number 5407). These also survived the test criteria, yet will not be used for IFOSTP as they exhibited too much damping (from 3.7% of critical at 5 psi to 4.05% of critical at 15 psi - approximately twice the damping as the #8556 airsprings for this particular system).

As shown from these tests, the airbags have performed well under the phase 3 conditions. These initial trials of the high frequency rig and airbags were very encouraging. Until the full IFOSTP test is running and the actual loading condition at each airbag can be monitored, further refinement of the loading spectrum for the durability tests is not possible.

8. Final Rig Configuration

Although the design phase made every effort to minimise the operating stress levels throughout the beam, fatigue cracking initiated in the weld attaching the beam to the base plate - consequently, the beam was replaced several times, with accompanying modifications to the beam-to-base attachment being performed each time. Figure 8 shows the final rig configuration, and it should be noted that the electromagnetic shaker has been replaced with an out-of-balance rotating mass unit, fixed to the top surface of the beam at the free end. This excitation method is driven by a speed controlled DC motor. A review of test methods led to this change, which still maintained unmanned operation of the rig (potential damage and costs to the electromagnetic shaker were high should the beam fracture while vibrating), and the tip displacements were no longer limited by the travel of the shaker sting. Also note

[4] Other airbags of the same type (ie: #8556) were subjected to phase 2 tests using a greater working pressure (2.5 psi to 35 psi cyclic range) than that in the original specification . The durability of these bags at these pressures have so far proven inadequate for IFOSTP requirements. Further discussion on a more representative overall test spectrum is still ongoing.

that the method of fixing the beam to the concrete block was changed from a welded attachment to a clamped arrangement (steel channels over the top of the beam bolted to the steel base plate). This serves to reduce stress concentrations otherwise induced by the welds, as well as allowing easier replacement of the beam.

9. Conclusion

The Aeronautical & Maritime Research Laboratory (AMRL) has developed a loading system to apply manoeuvre loads to the IFOSTP test article utilising airspring actuators. As these airsprings are to be subjected to the high frequency buffet simulation, a separate test rig was commissioned to test individual airspring durability under high frequency excitation and also to determine airspring damping.

A cantilever beam structure was chosen as a design for the rig, and two methods of sizing the rig were performed - a finite element method and an analytical approach. A comparison of results from the two methods proved favourable, leading to a final design for the test rig. The rig was shown to serve its purpose well in simulating the high frequency buffet conditions for testing of airspring actuators.

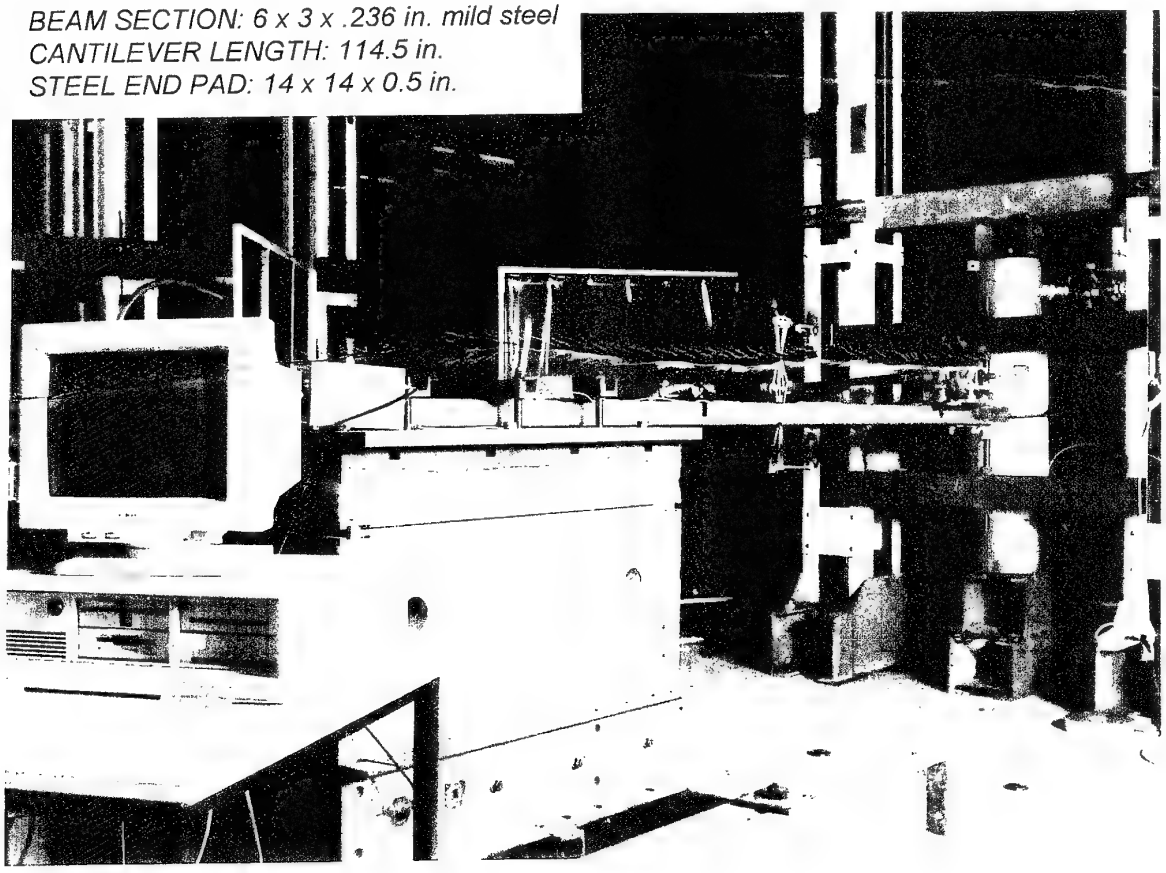

Figure 8: Final test rig configuration.

10. Acknowledgments

The author would like to greatly acknowledge the assistance of Dr. Pavel Trivailo, lecturer in Aerospace Engineering at the Royal Melbourne Institute of Technology (RMIT) for his contribution to this report. His work in producing the equations and explanations for the analytical solution of dynamic beam motion were invaluable in verifying the results of the FE model, which ultimately led to the construction of the high frequency test rig. The advice and assistance of all the AMRL staff associated with this project is also much appreciated, in particular Mr. Lorrie Molent for his guidance in FE modelling and Mr. Bob Dingley, Mr. Roy Bailey and Mr. Neil Manger for constructing the rig.

11. References.

1. Graham, D., Symons, D., Sherman, D. and Eames, T., "ARL F/A-18 IFOSTP Full Scale Fatigue Test", Proc. Fifth Australian Aeronautical Conference, Melbourne, 13 - 15 Sept. 1993, IEAust No. 93/6, (pp. 317-323), 1993.

2. Scanlon, R.W. and Prey, S.W., "F-18 Vibrational Environmental Analysis Report - Addendum 2 - Vertical Tail Dynamic Response Test and Analysis", MDA 4488, McDonnell Aircraft Company, St. Louis, USA, Dec 1985.

3. Hayes, P., Van Donkelaar, R., Kaye, R., "Development of a Rolling Sleeve Airspring", DSTO, AMRL, (to be published).

4. Meirovitch, L., "Elements of Vibration Analysis", 2nd ed., McGraw-Hill Book Company, Singapore, (pp. 220-227, 235-238), 1986.

5. Weaver, W.J., Timoshenko, S.P., Young, D.H., "Vibration Problems in Engineering", 5th ed., John Wiley & Sons, New York, USA. (pp. 428-429, 436-443), 1990.

6. Harris, C.M., "Shock and Vibration Handbook", 3rd ed., McGraw-Hill Inc., USA., (p 2-5), 1988.

This page intentionally left blank

Appendix 1 - PAFEC Data File.

```
TITLE CANTILEVER
C
CONTROL
PHASE=1
PHASE=4
PHASE=6
PHASE=7
PHASE=9
CONTROL.END
C
NODES
NODE.NUMBER       X       Y
1                 0       0
2                 4       0
3                 8       0
4                12       0
5                16       0
6                20       0
7                24       0
8                28       0
9                32       0
10               36       0
11               40       0
12               44       0
13               48       0
14               52       0
15               56       0
16               60       0
17               64       0
18               68       0
19               70       0
C
ELEMENTS
NUMBER     ELEMENT.TYPE    PROPERTIES      TOPOLOGY
 1            34000              1           1,2
 2            34000              1           2,3
 3            34000              1           3,4
 4            34000              1           4,5
 5            34000              1           5,6
 6            34000              1           6,7
 7            34000              1           7,8
 8            34000              1           8,9
 9            34000              1           9,10
 10           34000              1           10,11
 11           34000              1           11,12
 12           34000              1           12,13
 13           34000              1           13,14
 14           34000              1           14,15
 15           34000              1           15,16
 16           34000              1           16,17
 17           34000              1           17,18
 18           34000              1           18,19
C
BEAMS
SECTION.NUMBER     MATERIAL.NUMBER       IYY       IZZ     AREA     ZY      ZZ
      1                  12             18.412     6.057   4.025   6.137   4.038
 C
 MATERIAL
 MATERIAL.NUMBER         E              NU       RO
         12          29000000          .33     .0007
 C
 RESTRAINTS
 NODE       DIRECTION
 1           123456
 2           1345
 3           1345
 4           1345
 5           1345
 6           1345
 7           1345
 8           1345
 9           1345
 10          1345
 11          1345
 12          1345
 13          1345
 14          1345
 15          1345
 16          1345
 17          1345
 18          1345
 19          1345
 C
```

```
RESPONSE
TYPE.OF.RESPONSE     OUTPUT.TYPE
       1                    1
C
DAMPING
MODE=0
FREQUENCY      DAMPING.RATIO
    0                0.0
    35               0.0
C
FREQUENCIES.FOR.ANALYSIS
TYPE     START      FINISH     STEP
  1        0          35         1
C
SINE.LOADING
NODE.NUMBER     DIRECTION.OF.LOAD     TABLE.NUMBER
    10                   2                   1
C
TABLE.OF.APPLIED.FORCES
TABLE      BASIS.VALUE      VALUE.LIST
   1           0             600  0
   1           35            600  0
C
SINUSOIDAL.OUTPUT
NODE     DIRECTION
 10          2
 19          2
C
MASTERS
NODE.NUMBER     DIRECTION
  10               2
  19               2
C
MODES.AND.FREQUENCIES
AUTOMATIC.MASTERS
       60
C
END.OF.DATA
```

SCHEMATIC OF CANTILEVER BEAM MODEL.

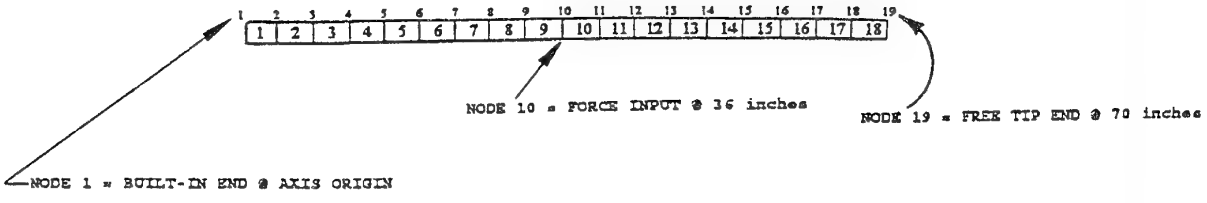

Appendix 2.

SECTION OF PAFEC DISPLACEMENT OUTPUT FILE (P = 600 lbf).

LOAD. CASE	FREQUENCY	NODE 10, DIRECTION 2 DISPLACEMENT	PHASE.ANGLE	NODE 19, DIRECTION 2 DISPLACEMENT	PHASE.ANGLE
1	.000	.5312E-01	360.0	.1284	360.0
1	1.000	.5318E-01	360.0	.1285	360.0
1	2.000	.5336E-01	360.0	.1290	360.0
1	3.000	.5366E-01	360.0	.1299	360.0
1	4.000	.5409E-01	360.0	.1311	360.0
1	5.000	.5465E-01	360.0	.1327	360.0
1	6.000	.5536E-01	360.0	.1346	360.0
1	7.000	.5622E-01	360.0	.1370	360.0
1	8.000	.5724E-01	360.0	.1399	360.0
1	9.000	.5845E-01	360.0	.1433	360.0
1	10.000	.5989E-01	360.0	.1473	360.0
1	11.000	.6155E-01	360.0	.1520	360.0
1	12.000	.6350E-01	360.0	.1574	360.0
1	13.000	.6577E-01	360.0	.1638	360.0
1	14.000	.6843E-01	360.0	.1712	360.0
1	15.000	.7157E-01	360.0	.1800	360.0
1	16.000	.7527E-01	360.0	.1904	360.0
1	17.000	.7970E-01	360.0	.2028	360.0
1	18.000	.8505E-01	360.0	.2178	360.0
1	19.000	.9160E-01	360.0	.2361	360.0
1	20.000	.9977E-01	360.0	.2591	360.0
1	21.000	.1102	360.0	.2884	360.0
1	22.000	.1240	360.0	.3269	360.0
1	23.000	.1428	360.0	.3797	360.0
1	24.000	.1701	360.0	.4564	360.0
1	25.000	.2131	360.0	.5770	360.0
1	26.000	.2905	360.0	.7942	360.0
1	27.000	.4703	360.0	1.299	360.0
1	28.000	1.350	360.0	3.767	360.0
1	29.000	1.397	180.0	3.942	180.0
1	30.000	.4450	180.0	1.270	180.0
1	31.000	.2593	180.0	.7493	180.0
1	32.000	.1803	180.0	.5276	180.0
1	33.000	.1366	180.0	.4049	180.0
1	34.000	.1089	180.0	.3272	180.0
1	35.000	.8978E-01	180.0	.2735	180.0

SECTION OF PAFEC DISPLACEMENT OUTPUT FILE (P = 1000 lbf).

LOAD. CASE	FREQUENCY	NODE 10, DIRECTION 2 DISPLACEMENT	PHASE.ANGLE	NODE 19, DIRECTION 2 DISPLACEMENT	PHASE.ANGLE
1	.000	.8854E-01	360.0	.2140	360.0
1	1.000	.8864E-01	360.0	.2142	360.0
1	2.000	.8894E-01	360.0	.2151	360.0
1	3.000	.8944E-01	360.0	.2165	360.0
1	4.000	.9015E-01	360.0	.2185	360.0
1	5.000	.9109E-01	360.0	.2211	360.0
1	6.000	.9226E-01	360.0	.2244	360.0
1	7.000	.9369E-01	360.0	.2284	360.0
1	8.000	.9541E-01	360.0	.2332	360.0
1	9.000	.9743E-01	360.0	.2388	360.0
1	10.000	.9981E-01	360.0	.2455	360.0
1	11.000	.1026	360.0	.2533	360.0
1	12.000	.1058	360.0	.2624	360.0
1	13.000	.1096	360.0	.2730	360.0
1	14.000	.1141	360.0	.2854	360.0
1	15.000	.1193	360.0	.3000	360.0
1	16.000	.1255	360.0	.3173	360.0
1	17.000	.1328	360.0	.3380	360.0
1	18.000	.1417	360.0	.3630	360.0
1	19.000	.1527	360.0	.3936	360.0
1	20.000	.1663	360.0	.4318	360.0
1	21.000	.1837	360.0	.4806	360.0
1	22.000	.2066	360.0	.5448	360.0
1	23.000	.2380	360.0	.6329	360.0
1	24.000	.2835	360.0	.7606	360.0
1	25.000	.3552	360.0	.9617	360.0
1	26.000	.4841	360.0	1.324	360.0
1	27.000	.7839	360.0	2.165	360.0
1	28.000	2.250	360.0	6.279	360.0
1	29.000	2.328	180.0	6.570	180.0
1	30.000	.7417	180.0	2.117	180.0
1	31.000	.4322	180.0	1.249	180.0
1	32.000	.3005	180.0	.8793	180.0
1	33.000	.2277	180.0	.6749	180.0
1	34.000	.1815	180.0	.5452	180.0
1	35.000	.1496	180.0	.4559	180.0

Appendix 3.

$$
\begin{aligned}
Y_i &= C_1(\cos k_i x + \cosh k_i x) + C_2(\cos k_i x - \cosh k_i x) \\
&+ C_3(\sin k_i x + \sinh k_i x) + C_4(\sin k_i x - \sinh k_i x)
\end{aligned}
$$

$$
\begin{aligned}
Y_i' &= C_1 k_i(-\sin k_i x + \sinh k_i x) + C_2 k_i(-\sin k_i x - \sinh k_i x) \\
&+ C_3 k_i(\cos k_i x + \cosh k_i x) + C_4 k_i(\cos k_i x - \cosh k_i x)
\end{aligned}
$$

$$
\begin{aligned}
Y_i'' &= C_1 k_i^2(-\cos k_i x + \cosh k_i x) + C_2 k_i^2(-\cos k_i x - \cosh k_i x) \\
&+ C_3 k_i^2(-\sin k_i x + \sinh k_i x) + C_4 k_i^2(-\sin k_i x - \sinh k_i x)
\end{aligned}
$$

$$
\begin{aligned}
Y_i''' &= C_1 k_i^3(\sin k_i x + \sinh k_i x) + C_2 k_i^3(\sin k_i x - \sinh k_i x) \\
&+ C_3 k_i^3(-\cos k_i x + \cosh k_i x) + C_4 k_i^3(-\cos k_i x - \cosh k_i x)
\end{aligned}
$$

Appendix 4.

$$(\cosh x)_{x=0} = \left(\frac{e^x + e^{-x}}{2}\right)_{x=0} = 1$$

$$(\sinh x)_{x=0} = \left(\frac{e^x - e^{-x}}{2}\right)_{x=0} = 0$$

$$\cosh x^2 - \sinh x^2 = 1$$

Appendix 5.

$$\boxed{\cos\beta L \cdot \cosh\beta L = -1}$$

$$\cos\beta L = \phi_1; \qquad -\frac{1}{\cosh\beta L} = \phi_2$$

The above equation is satisfied at: $\phi_1 = \phi_2$

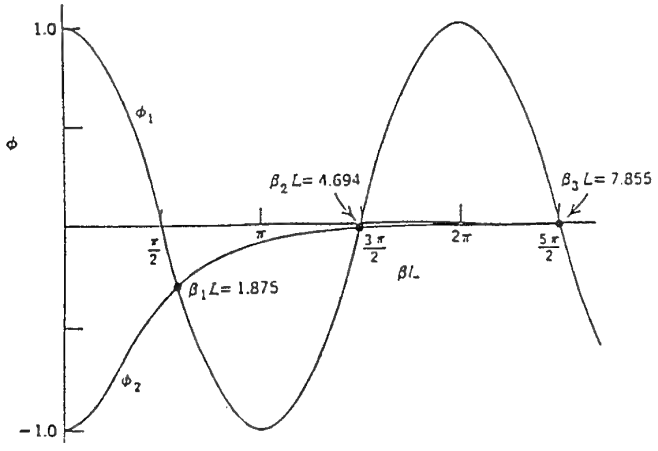

ANALYTICAL SOLUTION OF EQUATION (21)

$E = 29 \times 10^6\ psi$ $I = 6.057\ in^4$ *Beam length,* $x = l = 70\ in$ *Shaker @* $x_1 = 36\ in$ $A = 4.025\ in^2$ $\rho = 0.283\ lb/in^3$ $g = 386\ in/s^2$

$$\Delta = \left[(\cos k_i x - \cosh k_i x) + \alpha_i(\sin k_i x - \sinh k_i x)\right] \times \left[(\cos k_i x_1 - \cosh k_i x_1) + \alpha_i(\sin k_i x_1 - \sinh k_i x_1)\right]$$

$$\Theta = \left(\sin \Omega t - \frac{\Omega}{\omega_i}\sin \omega_i t\right)\left(\frac{1}{1-\Omega^2/\omega_i^2}\right)$$

Maximum Θ *occurs when* $\left(\sin \Omega t - \frac{\Omega}{\omega_i}\sin \omega_i t\right) = 1 \text{ or } -1.$

$$\omega_i = \frac{1}{2\pi}\frac{(k_i l)^2}{l^2}\sqrt{\frac{EIg}{\rho A}}$$

1 *i*	2 $k_i l$	3 α_i from eqn. (14)	4 B_i from "Mathematica" software	5 $B_i^2 l^4/(k_i l)^4$ from eqn. (21)	6 Δ term from eqn. (21)	7 *column 5 x column 6*	8 ω_i *Hz* eqn. (22)	9 Θ from eqn. (21) Ω=3Hz	10 Θ from eqn. (21) Ω=10Hz	11 Θ from eqn. (21) Ω=15Hz	12 Θ from eqn. (21) Ω=23Hz	13 Θ from eqn. (21) Ω=27Hz	14 Θ from eqn. (21) Ω=30Hz	15 Θ from eqn. (21) Ω=35Hz
1	1.875	-0.734096	0.119437	27711.81	1.42608	39519.258	27.86	1.012	1.148	1.408	3.140	16.452	-6.269	-1.729
2	4.694	-1.01847	0.119525	706.54	-2.82228	-1994.054	174.60	1.000	1.003	1.007	1.018	1.024	1.030	1.042
3	7.855	-0.999224	0.119513	90.08	-0.23777	-21.418	488.95	1.000	1.000	1.001	1.002	1.003	1.004	1.005
4	10.996	-1.00003	0.120065	23.67	2.64832	62.686	958.16	1.000	1.000	1.000	1.001	1.001	1.001	1.001
5	14.137	-0.999999	0.120648	8.75	0.48142	4.212	1583.74	1.000	1.000	1.000	1.000	1.000	1.000	1.000
6	17.279	-1.00000	0.121268	3.96	-1.37172	-5.432	2365.96	1.000	1.000	1.000	1.000	1.000	1.000	1.000

Below is an example of the calculated displacement given for driving frequency Ω = 23 Hz and P=600 lbf:

Each row in column #7 is multiplied by the corresponding row in column #12 as set out below:

39519.258 x *3.140* = *124090.4701*
-1994.054 x *1.018* = *-2029.9470*
-21.418 x *1.002* = *-21.4608*
62.686 x *1.001* = *62.749*
4.212 x *1.000* = *4.212*
-5.432 x *1.000* = *-5.432*

Total: *122100.5193*

The sum of the products (*122100.5193*) is then multiplied by P/EI (*3.416* x *10E-6*) to give the displacement which is *0.4171* inches.

Design and Development of a Test Rig for the High Frequency Testing of Rolling Sleeve Airsprings

G. Swanton

DSTO-TN-0001

DISTRIBUTION

AUSTRALIA

DEFENCE ORGANISATION

Defence Science and Technology Organisation

Chief Defence Scientist
FAS Science Policy
AS Science Corporate Management
} shared copy
Counsellor Defence Science, London (Doc Data Sheet only)
Counsellor Defence Science, Washington (Doc Data Sheet only)
Senior Defence Scientific Adviser (Doc Data Sheet only)
Scientific Advisor Policy and Command (Doc Data Sheet only)
Navy Scientific Adviser (3 copies Doc Data Sheet only)
Scientific Adviser - Army (Doc Data Sheet only)
Air Force Scientific Adviser

Aeronautical and Maritime Research Laboratory
Director
Library Fishermens Bend
Library Maribyrnong
Chief Airframes and Engines Division Division
Author: G. Swanton
D. Graham
D. Sherman
P. White
D. Symons
B. Madley
C. Martin
L. Molent
P. Hayes
R. Kaye

Electronics and Surveillance Research Laboratory
Director
Main Library - DSTO Salisbury

Defence Central

OIC TRS, Defence Central Library
Document Exchange Centre, DSTIC (8 copies)
Defence Intelligence Organisation
Library, Defence Signals Directorate (Doc Data Sheet Only)

Air Force

Aircraft Research and Development Unit
Tech Reports,CO Engineering Squadron,ARDU
AHQ CSPT
CLSA-LC
ASI-LC
TFPO-AF
TFLM SQD Williamtown
OIC ATF, ATS, RAAFSTT, WAGGA (2 copies)
TLO IFOSTP CANADA

UNIVERSITIES AND COLLEGES

Australian Defence Force Academy
Library
Head of Aerospace and Mechanical Engineering

OTHER GOVERNMENT DEPARTMENTS AND AGENCIES

AGPS

OTHER ORGANISATIONS

NASA (Canberra)

SPARES (6 COPIES)

TOTAL (47 COPIES)

AL 149 DEPARTMENT OF DEFENCE

PAGE CLASSIFICATION
UNCLASSIFIED

PRIVACY MARKING

DOCUMENT CONTROL DATA

1a. AR NUMBER	1b. ESTABLISHMENT NUMBER	2. DOCUMENT DATE	3. TASK NUMBER
AR-009-201	DSTO-TN-0001	FEBRUARY 1995	AIR 88/053

4. TITLE

DESIGN AND DEVELOPMENT OF A TEST RIG FOR THE HIGH FREQUENCY TESTING OF ROLLING SLEEVE AIRSPRINGS

5. SECURITY CLASSIFICATION (PLACE APPROPRIATE CLASSIFICATION IN BOX(S) IE. SECRET (S), CONF. (C) RESTRICTED (R), LIMITED (L), UNCLASSIFIED (U)).

DOCUMENT	TITLE	ABSTRACT
U	U	U

6. NO. PAGES: 28

7. NO. REFS.: 6

8. AUTHOR(S)

G. SWANTON

9. DOWNGRADING/DELIMITING INSTRUCTIONS

Not applicable.

10. CORPORATE AUTHOR AND ADDRESS

AERONAUTICAL AND MARITIME RESEARCH LABORATORY
AIRFRAMES AND ENGINES DIVISION
PO BOX 4331
MELBOURNE VIC 3001 AUSTRALIA

11. OFFICE/POSITION RESPONSIBLE FOR:

RAAF ASI-LC

SPONSOR _____

SECURITY _____

DOWNGRADING _____

CAED

APPROVAL _____

12. SECONDARY DISTRIBUTION (OF THIS DOCUMENT)

Approved for public release.

OVERSEAS ENQUIRIES OUTSIDE STATED LIMITATIONS SHOULD BE REFERRED THROUGH DSTIC, ADMINISTRATIVE SERVICES BRANCH, DEPARTMENT OF DEFENCE, ANZAC PARK WEST OFFICES, ACT 2601

13a. THIS DOCUMENT MAY BE ANNOUNCED IN CATALOGUES AND AWARENESS SERVICES AVAILABLE TO ....

No limitations.

14. DESCRIPTORS

High frequencies	Airbags	Rolling sleeve
F/A-18 aircraft	Structural tests	
Fatigue tests	Actuators	
Manoeuvre loads	Damping	

15. DISCAT SUBJECT CATEGORIES

16. *ABSTRACT*

AMRL's F/A-18 IFOSTP fatigue test has introduced several new concepts in the field of aircraft structural testing. One of the innovations has been the development of the pneumatic actuator or "rolling sleeve" airspring for the application of aircraft manoeuvre loads. These airsprings have been subjected to several preliminary acceptance test phases, one of which simulated the effects of high frequency buffet loads. This report details the design and implementation of the test rig developed to conduct this type of testing.

PAGE CLASSIFICATION
UNCLASSIFIED
PRIVACY MARKING

THIS PAGE IS TO BE USED TO RECORD INFORMATION WHICH IS REQUIRED BY THE ESTABLISHMENT FOR ITS OWN USE BUT WHICH WILL NOT BE ADDED TO THE DISTIS DATA UNLESS SPECIFICALLY REQUESTED.

16. ABSTRACT (CONT).

17. IMPRINT

AERONAUTICAL AND MARITIME RESEARCH LABORATORY, MELBOURNE

18. DOCUMENT SERIES AND NUMBER	19. WA NUMBER	20. TYPE OF REPORT AND PERIOD COVERED
DSTO Technical Note 0001	28-203A	

21. COMPUTER PROGRAMS USED

22. ESTABLISHMENT FILE REF.(S)

M1/9/38

23. ADDITIONAL INFORMATION (AS REQUIRED)